JOURNAL OF GEOPHYSICAL RESEARCH, VOL. 113, C04003, doi:10.1029/2007JC004298, 2008

Stacked jets in the deep equatorial Atlantic Ocean

Carsten Eden[1] and Marcus Dengler[1]

Received 20 April 2007; revised 5 October 2007; accepted 2 January 2008; published 3 April 2008.

[1] Middepth current measurements in the equatorial Atlantic are characterized by elevated levels of energy contained in zonal flows of high baroclinic mode number. These alternating zonal flows, often called equatorial stacked jets, have amplitudes up to 20 cm s^{-1} and vertical wavelengths of 600 m. The jets are most pronounced in the depth range between 500 and 2500 m. Repeated direct velocity observations at 35°W indicate that the jets are coherent within ±1° of the equator. Individual jets can persist for 1–2 years, but they appear and decay rather irregularly. The equatorial stacked jets are also found in realistic general circulation model simulations. The features grow in amplitude with increasing horizontal and vertical model resolution. However, even at very high model resolutions, their amplitudes are still underestimated. In all model simulations, high levels of energy related to the stacked jets are found in the vicinity of the western boundary currents (WBCs). Depth range and strength of the WBCs in different experiments are related to depth range and strength of the jets. In the interior, stacked jets are characterized by eastward wave propagation suggesting that high baroclinic mode Kelvin waves radiate energy generated in the WBC into the interior and form the stacked jets.

Citation: Eden, C., and M. Dengler (2008), Stacked jets in the deep equatorial Atlantic Ocean, *J. Geophys. Res.*, *113*, C04003, doi:10.1029/2007JC004298.

1. Introduction

[2] Stacked jets are equatorially trapped zonal flows with short vertical scales that have been observed in all tropical oceans. They were first discovered by *Luyten and Swallow* [1976] in current observations from the Indian Ocean. *Hayes and Milburn* [1980], *Leetma and Spain* [1981], and *Eriksen* [1981] reported similar features in the Pacific Ocean while the existence of the jets in the Atlantic Ocean was first inferred from hydrographic data by *Eriksen* [1982]. *Ponte and Luyten* [1990] confirmed their existence in the Atlantic Ocean using a direct current profile at the equator. All observations characterize the stacked jets as strong zonal flow of alternating sign with amplitudes up to 20 cm s^{-1} found at depths down to about 3000 m. The alternating zonal flow forming the stacked jets is organized in pancake-like structures with typical vertical scales of 100–400 m trapped within ±1° of the equator.

[3] While the meridional and vertical structure of the jets are reasonable well defined, the zonal and temporal scales of the jets are less well observed. *Firing* [1987] and *Ponte and Luyten* [1989] found the stacked jets in the Pacific Ocean to be stationary for periods of 1 year or longer and zonal extent of the jets of at least 10° of longitude. For the stacked jets in the Atlantic, direct velocity observations by *Gouriou et al.* [2001] suggested a zonal extent of at least 25°. For the same ocean, *Send et al.* [2002] reported a zonal extent of 10° and a timescale associated with the persistence of individual jets of at least 1 year. In their data, no seasonal cycle was apparent, but interannual variability of the jets was strongly pronounced. *Johnson and Zhang* [2003] diagnosed a period of about 5 years and a zonal wavelength of 70° (±60°) from an extensive CTD data set. However, *Gouriou et al.* [1999] and *Schmid et al.* [2005] found from velocity profiles repeated within a few months that at a given depth, jets can have opposing directions.

[4] CFC measurements have revealed that within the eastward cores of the stacked jets, relatively recently formed North Atlantic Deep Water (NADW) arriving at the western boundary from the subpolar North Atlantic, is advected to the eastern equatorial Atlantic [*Weiss et al.*, 1985; *Gouriou et al.*, 2001; *Bourlès et al.*, 2003]. Positive correlation between CFC-11 concentration and stacked jets (with high concentration in eastward cores and low concentration in westward cores) were reported as far east as 10°W by *Gouriou et al.* [2001]. These results further suggest a high zonal coherence and long timescales of the jet cores and imply a possible role of the stacked jets for the ventilation of the interior equatorial Atlantic.

[5] The mechanism responsible for the stacked jets is still under debate. *Wunsch* [1977] and *McCreary* [1984] proposed a linear equatorial wave response of high baroclinic modal structure driven by seasonally varying surface forcing. *Ponte* [1989] considered linear equatorial waves with short vertical scales generated by temporal variability of deep western boundary currents. The linear theories, however, appear unsatisfactory in explaining the vertical and horizontal scales and the irregular temporal behavior of the jets.

[1]IFM-GEOMAR, Kiel, Germany.

0148-0227/08/2007JC004298$09.00

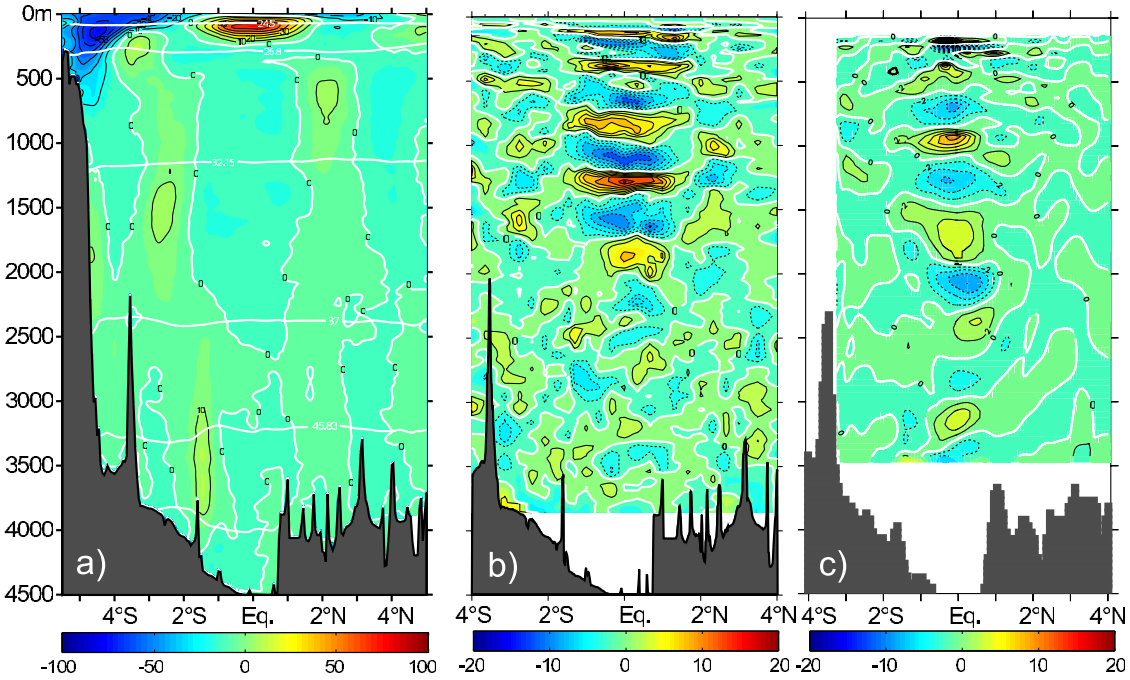

Figure 1. (a) Mean zonal flow at 35°W determined from 16 repeat sections. Color contours change every 5 cm s^{-1} while black contour lines indicate changes in velocities of 10 cm s^{-1}. (b) Instantaneous zonal velocity section as observed in May 2003 from which the zonal flow of the first nine vertical modes has been removed. Stations spacing was 1/3° within 2° of the equator and 1/2° elsewhere. Color contour interval is 2 cm/s, while black lines separate velocities increased by 5 cm/s. Data from depths below 3850 m are not displayed. (c) Instantaneous zonal velocity from which the first nine vertical modes has been removed in a model simulation (experiment 1/12−94). Contour interval is identical to Figure 1b.

[6] In recent years nonlinear mechanisms have also been proposed to explain the stacked jets. *Muench and Kunze* [1999] and *Muench and Kunze* [2000] showed that energy can be transferred from the internal wave field to the equatorial stacked jets by momentum flux divergence in vertical critical layers (given by the large-scale flow). This process could thus sustain the stacked jets despite energy loss due to dissipation within the jets and energy reflection at meridional boundaries. *Hua et al.* [1997] suggest symmetric instability of the large-scale mean flow to generate the stacked jets. Symmetric instability is a well known feature in convective situations of the atmosphere [*Emanuel*, 1994] and the ocean [*Haine and Marshall*, 1998]. Near the equator, however, zonal flow in the stratified interior can also become symmetrically unstable, when the horizontal (or vertical) shear of the flow is sufficiently strong (and of required sign) [*Stevens*, 1983]. *Send et al.* [2002] found some observational support of this mechanism, although it remained unclear if the shear of the mean flow (or its seasonal cycle) in the interior of the ocean becomes strong enough to achieve significantly large growth rates of the instability [*d'Orgeville et al.*, 2004]. Furthermore, simple symmetric instability theory predicts that the fastest growing modes are those with infinite vertical wave number in disagreement with observations.

[7] More recently, B. L. Hua et al. (Destabilization of mixed rossby gravity waves and equatorial zonal jets formation, submitted to *Journal of Fluid Mechanics*, 2008) pointed out that since short Rossby and Yanai waves are unstable against perturbations [*Gill*, 1974], they may interact with long high baroclinic mode Kelvin waves, forming the observed stacked jets. Hua et al. (submitted manuscript, 2008) describe how such an instability can lead to an energy transfer from short (Yanai and Rossby waves) to large (high baroclinic mode Kelvin waves, i.e., stacked jets) horizontal scales, indicative of an inverse energy cascade, i.e., putting the stacked jets into the context geostrophic turbulence.

[8] Here we revisit the equatorial stacked jets using both observational results and numerical model simulations. Using a large database of available direct current observations at 35°W, we are able to confidently describe the characteristic horizontal, vertical and temporal scales of the jets in the western equatorial Atlantic Ocean in the following section. In section 3 we discuss realistic general circulation model simulations with very high vertical resolution, that are beginning to show high baroclinic mode flow features that are comparable to the observed stacked jets. Possible generation mechanisms of the stacked jets are assessed using sensitivity experiments with the numerical models and are discussed in section 4. Finally, a summary and a discussion of our conclusions is presented in the last section.

2. Observed Structure of the Stacked Jets

[9] The mean zonal circulation in the equatorial Atlantic exhibits a rather complex zonal current structure, in particular at middepth. This is illustrated in Figure 1a where the mean circulation at 35°W compiled from observations from 16 individual ship surveys carried out between 1990 and

Table 1. Vessel and Date of the 35°W Section Occupation[a]

Vessel (Leg)	Date	Profiles	Instrument
Meteor (M14/2)	10/1990	4	Pegasus
Meteor (M16/3)	06/1991	13	Pegasus, LADCP
Meteor (M22/2)	11/1992	10	Pegasus, LADCP
Meteor (M27/3)	03/1994	12	Pegasus, LADCP
Edwig Link (Etambot 2)	04/1996	10	LADCP
La Thalassa (Equalant)	08/1999	16	LADCP
Meteor (M47/1)	04/2000	14	LADCP
Sonne (152)	12/2000	14	LADCP
Meteor (M53/2)	05/2002	14	LADCP
Sonne (171)	05/2003	14	LADCP

[a]Additionally, number of profiles within 2° of the equator and the profiling instrument are listed.

2005 is presented. The reader is referred to *Hormann and Brandt* [2007] and *Schott et al.* [2003] for details of the composition. The repeat cruises that sampled the whole water column are listed in Table 1. This data set is also used for the analysis below. The baroclinic structure of the mean flow (Figure 1a) appears to be dominated by the first few baroclinic vertical modes. Note that there is also a large annual cycle superimposed on the mean flow which is, similar to the mean flow, also dominated by the first and second baroclinic vertical mode [*Brandt and Eden*, 2005]. Also superimposed on the mean low-baroclinic-mode flow and its annual cycle are energetic, alternating currents at much smaller vertical scale that were observed in all of the individual ship sections (see Table 1). An example in Figure 1b shows the zonal flow from a direct velocity section measured in May 2003, from which the first nine vertical baroclinic modes have been removed. Note that the modal decomposition is used here as a method of scale separation; its dynamical relevance is questionable. (In the presence of a sloping bottom and strong background flow the simple modal decomposition as chosen here is formally inapplicable.)

[10] The high baroclinic mode zonal flow in Figure 1b represents a series of vertically stacked jets with amplitudes of 5–15 cm s^{-1}. These jets are confined to within 100–200 km of the equator and have a vertical wavelength of a few hundred meters that increases with depth. They are most pronounced in the depth range from a few hundred meters to about 3000 m depth. Note that in the work of *Send et al.* [2002], analyzing a subset of the current profiles shown here, it was found that the stacked jets begin to show up in vertical mode number 8 and higher and that the jets can be viewed best in the ship sections by removing the first nine vertical modes. This was found to be valid here as well and is therefore not discussed further.

[11] For a more quantitative description of the stacked jets in the Atlantic Ocean, we use WKBJ-scaled and vertically ''stretched'' zonal velocity profiles to compute vertical wave number spectra and meridional coherence. WKBJ-scaled profiles refer to a stretched vertical coordinate ($z^* = \int_z^0 dzN(z)/N_0$) and scaled velocities ($u^* = \sqrt{N_0/N_{(z)}}\, u$) to account for the dependence on stratification of solutions to the vertical structure equation. The effect of the transformation is that the properties of wave-like structures, such as the stacked jets, are more stationary with depth. (Note that the WKBJ approximation is formally valid only for wavelengths small compared to the scale on which N varies.) The procedure is applied to all profiles collected at 35°W listed in Table 1. To highlight features of the stacked jets, the depth range of the analysis is limited to 500–3000 m. For the scaling, we used the time mean $N(z)$ profile calculated from all CTD collected within 2° of the equator, while for N_0, the average stratification $\bar{N}(z) = 1.71 \times 10^{-3}$ s^{-1} between 500 m and 3000 m was used. Integration started at 500 m which was also taken as reference depth (z_0^*).

[12] The variance preserving vertical wave number spectrum of scaled zonal velocity shows a pronounced peak at a stretched wavelength of 625 m for profiles from the region 0.5°S to 0.5°N (red line in Figure 2a). In terms of vertical modes of a resting-ocean, flat-bottom decomposition, this wavelength corresponds to modes 14 through 16. In the same latitude band, elevated energy is also found for wavelength of 833 m and 500 m while profiles from the intervening regions 1.5–2.5°S and 1.5–2.5°N (green line) show no spectral peak. For the regions in between (black and blue lines), a transition between these two extreme situations is observed, with the tendency for larger vertical wavelengths off the equator. Meridional coherence of the individual profiles from each cruise with the respective profile from the equator for wavelengths of 625 m and 500 m is statistically significant for all profiles from within 1° of the equator (Figure 2b). For wavelengths 825 m and 416 m, coherence is significant only within 0.5° of the equator. The observations at 35°W thus indicate that the stacked jets are confined to within one degree of the equator and exhibit maximum energy at a vertical wavelength of about 625 m.

[13] The temporal variability of the stacked jets becomes obvious in Figure 3 where the scaled zonal velocity profiles from the equator from all available ship sections are displayed. Individual jets seem to persist for 1–2 years, i.e., can be seen in up to three sequential cruises, but no such feature is observed to persist for more than 2 years. Furthermore, as has been noted by *Schmid et al.* [2005] from a similar data set, there is no pair of sequential profiles with matching jets throughout the whole water column. In the work of *Send et al.* [2002], a similar result concerning the life time of the stacked jets in the equatorial Atlantic was obtained based on velocity time series from a mooring deployed on the equator in the western tropical Atlantic and from several individual ship sections (a subset of the data used here).

3. Simulated Stacked Jets

[14] Equatorial stacked jets can also be found in numerical models. In this study, four different general circulation model versions of the Atlantic Ocean are discussed, differing in their horizontal (1/3° versus 1/12°) and vertical (45, 94, and 450 levels) resolution, as summarized in Table 2. The set up of experiment 1/3–45 is comparable to standard eddy-permitting models covering the North Atlantic from 20°S to 70°N and is also discussed by, e.g., *Eden and Oschlies* [2006] (their experiment BIHARM). Experiment 1/12–45 is a typical eddy-resolving model setup and differs from 1/3–45 by the increased (eddy-resolving) horizontal resolution and reduced sub-grid-scale damping. More details about both model setups can be found in the work of *Eden and Oschlies* [2006] and *Eden* [2006]. Both setups

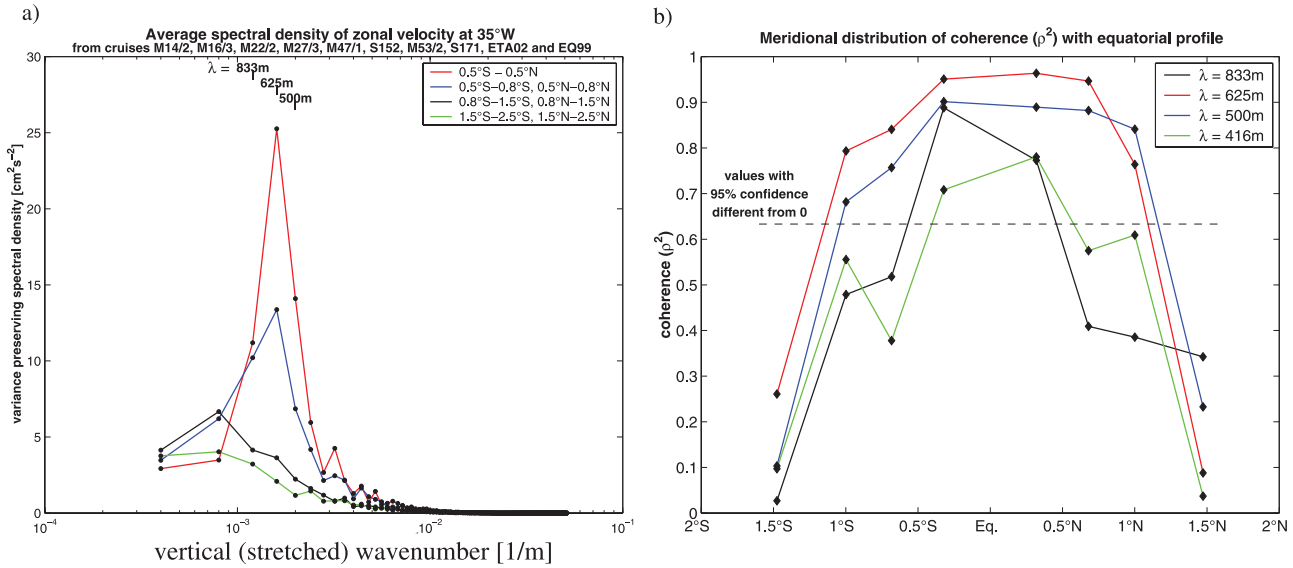

Figure 2. (a) Variance preserving vertical wave number spectrum in stretched vertical coordinates from 35°W determined from the velocity profiles of the cruises given in Table 1 within the indicated latitudinal band (colored lines). (b) Meridional coherence of profiles off the equator with the equatorial profile of the individual ship cruises as a function of latitude for the indicated stretched vertical wavelength (colored lines). The dashed line denotes nonzero coherence at a 95% significance level.

share identical vertical resolution (45 levels) which is standard for state-of-the-art ocean models (or slightly higher). In the depth range of the thermocline the vertical resolution decreases from approximately 70 m at a depth of 500 m to 250 m at a depth of 2500 m. Note that a vertical wavelength of the stacked jets (approximately 500 m) is thus only barely resolved by this vertical grid, i.e., only by a couple of grid points. Therefore, the simulated stacked jets

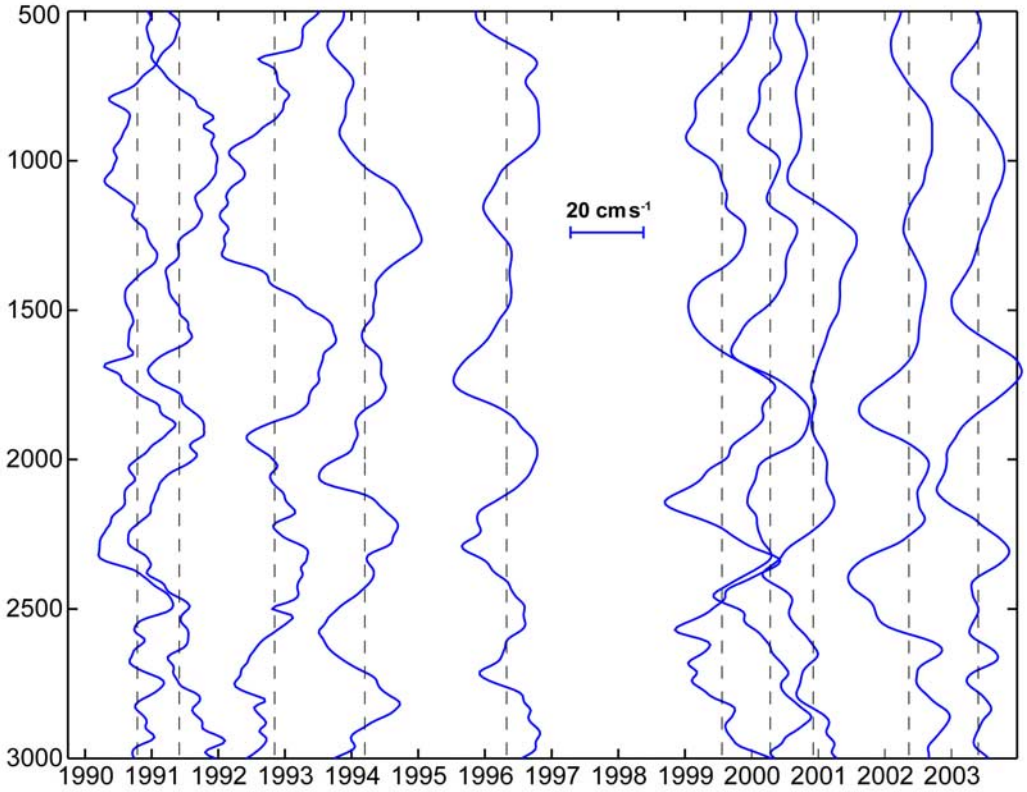

Figure 3. Stretched zonal velocity profiles at the equator for all available ship cruises as listed in Table 1. Individual profiles are shifted to indicated their location in time. The dashed lines correspond to zero velocity.

Table 2. Names of Model Experiments and Most Important Features of the Respective Model Setup

Exp. Name	Horizontal Resolution	Levels	Highest/Lowest Vertical Resolution	Horizontal Domain
1/3–45	1/3° × 1/3°	45	10 m/250 m	20°S–70°N
1/3–450	1/3° × 1/3°	450	1 m/25 m	12°S–12°N
1/12–45	1/12° × 1/12°	45	10 m/250 m	20°S–70°N
1/12–94	1/12° × 1/12°	94	10 m/50 m	12°S–12°N

on the standard, 45-level vertical grid should be viewed with caution, since the results might be contaminated by numerical grid noise, wave dispersion errors, etc. Such artifacts have indeed been identified in numerical models and are discussed by, e.g., *Weaver and Sarachik* [1990].

[15] In order to overcome this numerical issue, two additional model experiments are discussed here: an eddy-permitting setup with 1/3° horizontal resolution identical to 1/3–45 but with a vertical resolution increased by a factor 10 at each depth (experiment 1/3–450), and an eddy-resolving setup with 1/12° horizontal resolution and 94 vertical levels having 10 m thickness at the surface, increasing to 50 m at and below 250 m (experiment 1/12–94). By using increased vertical resolution, we are able to assure that the vertical scale of the simulated stacked jets is well separated from the vertical grid scale. Note also that lateral and vertical diffusivity and viscosity remained unchanged in the experiments with higher vertical resolution compared to the respective lower resolution experiments. Therefore, the jets in the experiments 1/12–94 and 1/3–450 should be less affected by numerical problems. In the following, we thus assume that the simulated jets are not generated by numerical noise.

[16] The horizontal domain of the models differ as well. While the experiments with the standard vertical grid (45 levels) span the North Atlantic from 20°S to 70°N, the model versions with increased vertical resolution cover only the tropical Atlantic from 12°S to 12°N. In all cases, however, open boundary conditions [*Stevens*, 1990] are used at the northern and southern boundaries of each model domain. For inflow conditions (calculated from a wave radiation condition [*Stevens*, 1990]) at those open boundaries, temperature and salinity taken from a combination of the climatologies of *Boyer and Levitus* [1997] and *Levitus and Boyer* [1994] (serving also as the initial conditions of all models) are prescribed. Note that to a large extent, the inflow boundary conditions determine the location and strength of the deep western boundary current (DWBC) and the meridional overturning circulation. All models are integrated for a 10 year spinup period, the results shown here are taken from a subsequent integration of the models of 10 years.

[17] Similar to the observations, a stacked jet structure develops in all model simulations (Figure 1c). Note that in the model simulation 1/12–94 (Figure 1c) the vertical wavelength of the stacked jets is well resolved, in contrast to the models with 45 levels only, giving confidence that the high baroclinic mode structure visible in Figure 1c is not caused nor affected greatly by numerical artifacts. On the other hand, the model versions with the standard vertical grid with 45 levels also show such stacked jet-like flow structure, albeit with smaller amplitudes.

[18] In all simulations, the distribution of variance of high baroclinic mode zonal flow along 35°W (Figures 4a–4d) exhibits elevated energy concentrated in a narrow strip at the equator. This energy increases with increased vertical resolution in the simulations. While the increase in horizontal resolution does not seem to affect the level of energy in the two models with the standard vertical grid with 45 levels, the energy clearly increases at increased horizontal resolution when going to higher vertical resolution. However, it should be noted that the level of variance in the model simulations is still low compared to the observations: Figure 4e shows that variance reaches 5–15 $cm^2\ s^{-2}$ at the equator in the observations, while in the simulations it is consistently below 5 $cm^2\ s^{-2}$ even in experiment 1/12–94, the model version with the highest level of energy. Furthermore, the observations also indicate elevated variance at 2–2.5° off the equator that is not reproduced in the different model simulations.

4. Mechanism Generating Stacked Jets

[19] All simulations show southward flow crossing the equator at the western boundary below about 1000–1500 m depth associated with the deep western boundary current (DWBC) (Figure 5). Above the DWBC, there is northward flow across the equator associated with the North Brazil Current (NBC). The magnitude of the mean western boundary currents (WBC) ranges between 10 to 40 cm s^{-1}, with stronger flow in the model versions having higher horizontal resolution. The depth of the NBC and the DWBC cores vary in different models. Note that this is predominantly due to the different model domains: While the inflow of the DWBC in the model versions covering only the tropical Atlantic is governed by the density structure prescribed at inflow points at the open boundaries, the DWBC in the basin wide models tend to be shallower compared to observations. This results in a deeper DWBC in the regional models compared to the basin wide model version. Note that simulated DWBCs appearing at shallower depths than observed are a well known artifact due to biases in water-mass characteristics resulting from erroneous diapycnal mixing and model biases in the ventilation of the subpolar North Atlantic.

[20] A pronounced zonal gradient of high baroclinic mode variance with enhanced energy towards the west and a maximum at the depth levels of the WBCs is indicated in all simulations (Figure 5). In fact, the simulations suggest a correlation between the strength and location of the WBCs and the middepth maximum of variance contained in high baroclinic mode zonal flow: While the level of variance tends to be higher in the models with higher horizontal resolution and stronger WBC, a shallower or deeper DWBC leads to a corresponding change in depth of the energy maximum. Note that in experiment 1/12–94, and, to a lesser extent in experiment 1/3–450, there is also a shallow local maximum in high baroclinic mode energy related to the northward flowing NBC, which reaches deeper at the equator in the regional models compared to the basin wide model version.

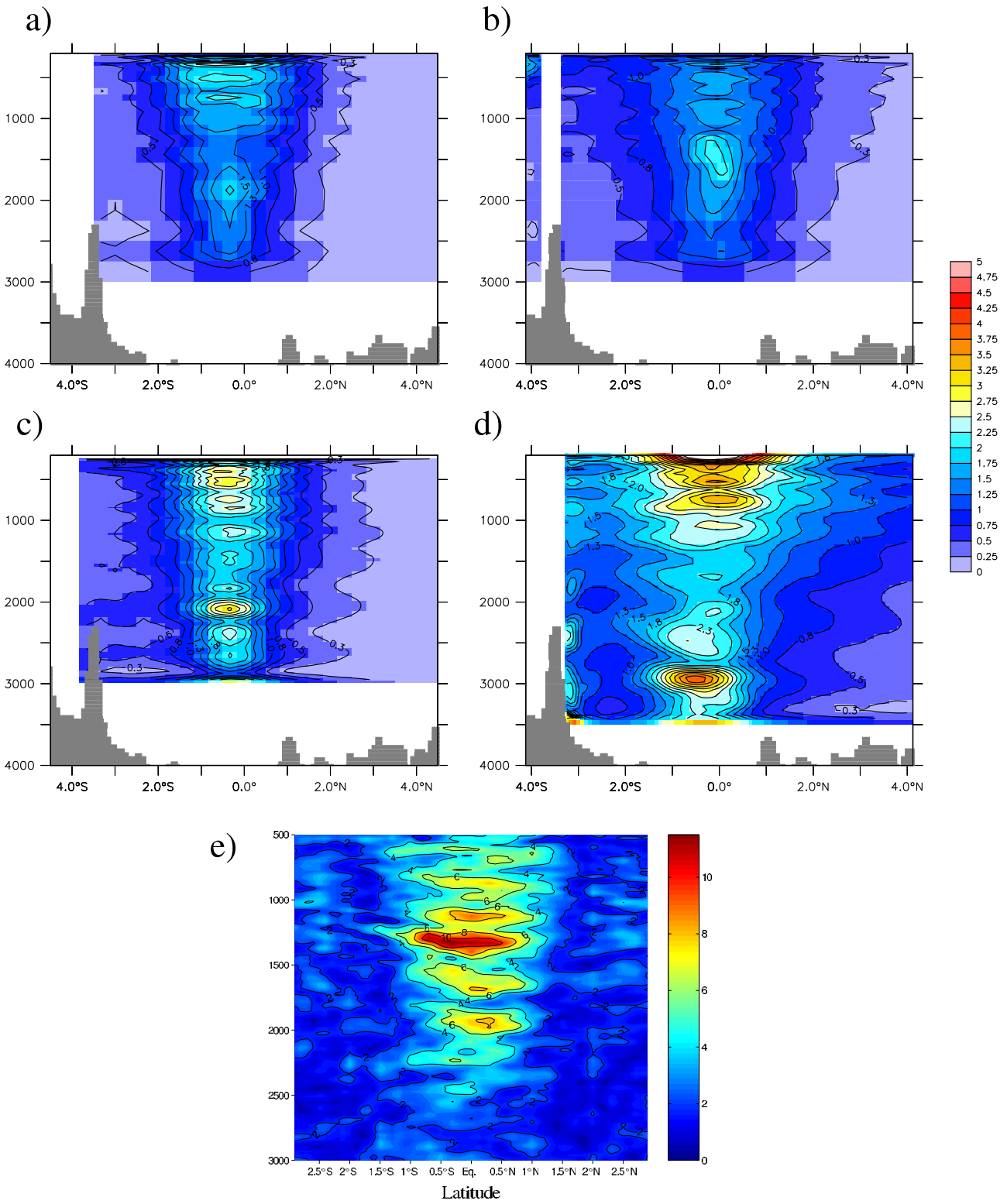

Figure 4. Variance (over time) in $cm^2\ s^{-2}$ of the zonal velocity from which the first nine vertical modes have been removed at 35°W for model experiment (a) 1/3–45, (b) 1/12–45, (c) 1/3–450, and (d) 1/12–94 and (e) from the observations listed in Table 1. Note the different color scale in Figure 4e.

[21] Time series of high baroclinic mode zonal flow at the equator show velocity fluctuations that are propagating predominantly to the east, indicative of Kelvin waves (Figure 6). Their wave speeds are roughly 2000 km/180 days ≈13 cm/s. For a constant stratification of $\bar{N}_0 = 1.71 \times 10^{-3}\ s^{-1}$ (as used above for the observations) and a water depth of $h = 3000$ m, this corresponds to a gravity or Kelvin wave speed of the 12. vertical mode, a reasonable value for

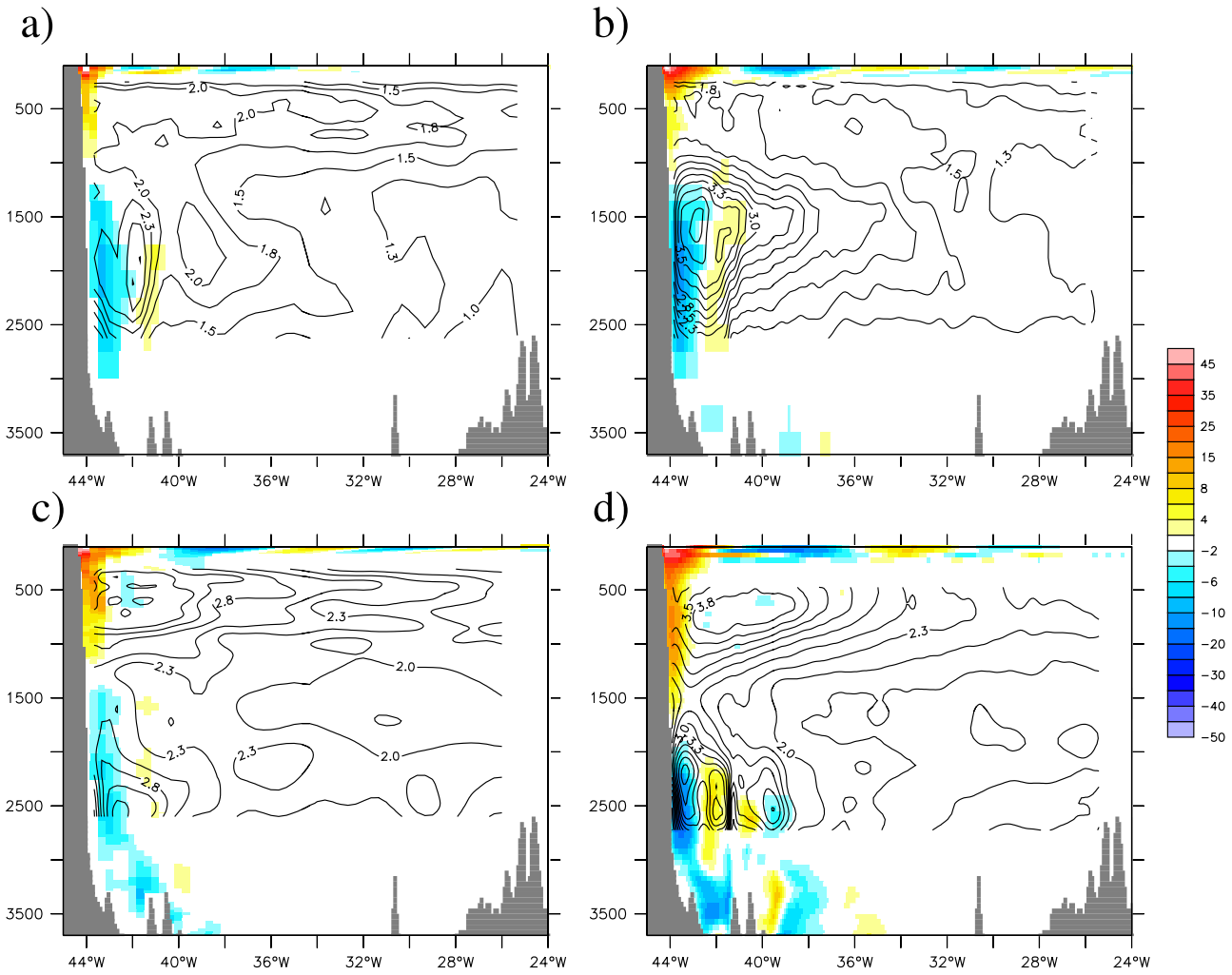

Figure 5. Mean meridional velocity (color) along the equator in cm s^{-1} in model experiment (a) 1/3–45, (b) 1/12–45, (c) 1/3–450, and (d) 1/12–94. Superimposed as contour lines is the energy contained in the high baroclinic modes, i.e., the variance (in time) in $cm^2\ s^{-2}$ of the zonal velocity from which the first nine vertical modes have been removed. Note that the variance is not shown for the complete depth range.

a high baroclinic Kelvin wave speed that is consistent with the above analysis, although slightly larger when compared to the observations, where the energy of the stacked jets peak at mode number 14–16. Note that similar eastward propagating structures can be found at different depths in all model simulations (not shown).

[22] *Hua et al.* [1997] suggested a shear instability of the large scale flow field at the equator as a formation mechanism for the stacked jets. A simple requirement for a sheared zonal flow to become unstable is that the Ertel potential vorticity becomes zero, i.e., that $fQ \leq 0$ where Q denotes potential vorticity and f the Coriolis parameter. Linear growth rates of inviscid particle displacements are given by $\omega^2 = -Qgf/N^2$ [*Haine and Marshall*, 1998].

[23] In the case of such a so-called symmetric instability, a zonally constant zonal mean flow is considered (as, e.g., in the work of *Hua et al.* [1997]). It is only the meridional (or vertical) shear of the zonal mean current which contributes to Q and which causes the instability. In the realistic model, however, the mean flow is neither zonal nor zonally constant. In particular the energetic DWBC is flowing southeastward across the equator and, furthermore, it is not constant but highly fluctuating, in agreement with observations [*Schott et al.*, 1993]. Therefore, it is clear that the simple linear theory of symmetric instability cannot be applied directly to the realistic model.

[24] However, as before for the vertical modal decomposition, we continue to ignore such complications and apply the necessary condition fQ and growth rates ω using the potential vorticity calculated from the instantaneous zonal and meridional velocity, i.e., using $Q = \rho_0^{-1}(u_z\rho_y - v_z\rho_x + \rho_z(v_x - u_y + f))$. Although different from the idealized situation of a sheared zonal mean flow in symmetric instability theory, fQ and ω estimated in this way, might at least give a rough estimate (which we shall call "effective" below) of the "real" value (currently inaccessible for theoretical considerations) of these quantities in the more complicated situation of the realistic model. We shall therefore assume that a large effective ω points toward the importance of symmetric instability of the equatorial flow.

[25] In our model simulations, the effective necessary condition for symmetric instability is often fulfilled near

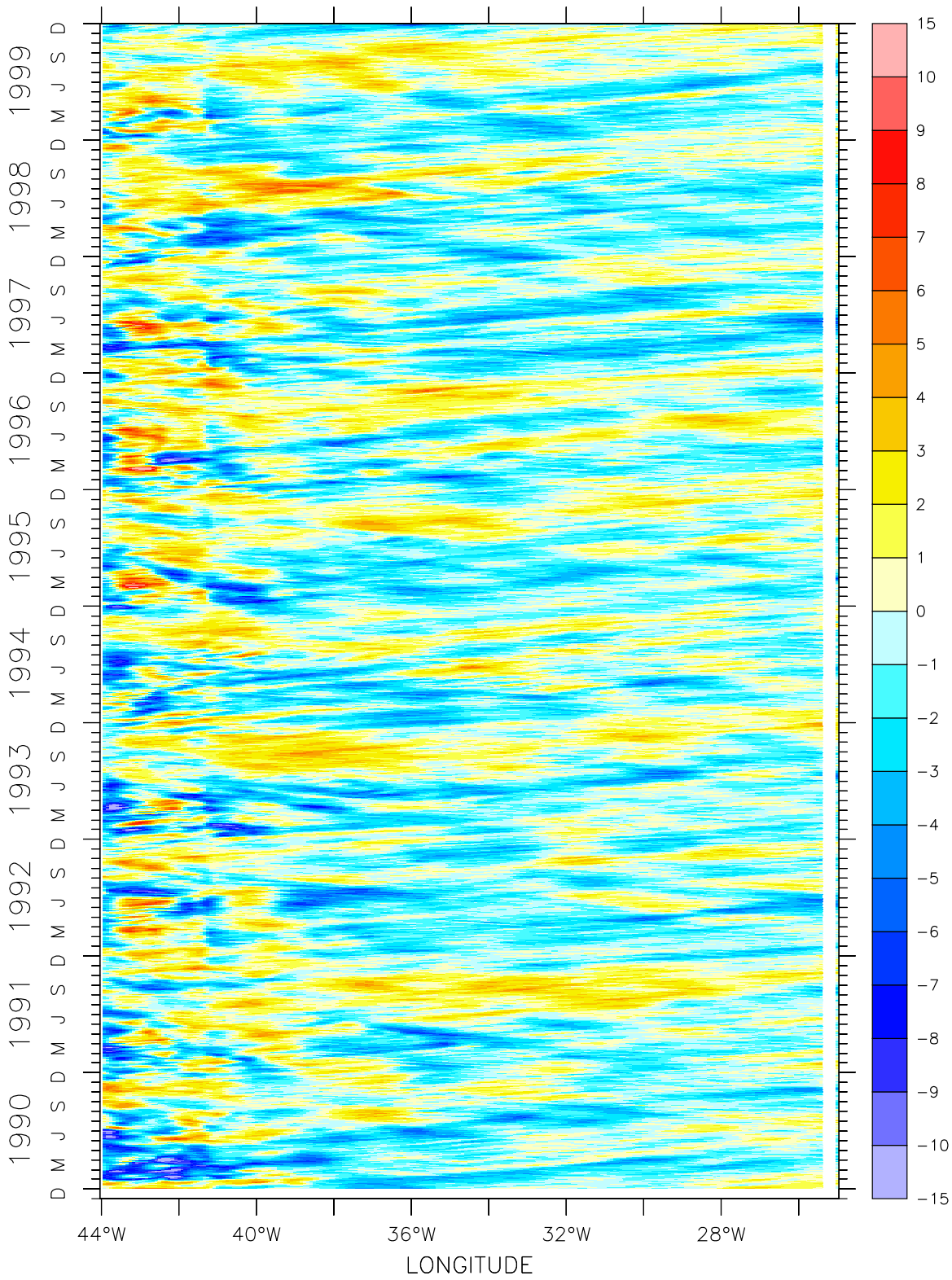

Figure 6. Zonal velocity in cm s^{-1} from which the first nine vertical modes have been removed at 2000 m depth in experiment 1/12−94.

the equator. Here, f becomes small and the magnitude of the background shear, in most cases dominated by u_y (not shown) is comparable to f and signed such that Q can become zero. In fact, the effective growth rates near the equator can become quite large. Note that off the equator, fQ becomes only rarely negative (mostly in convective situations with $\rho_z \rightarrow 0$) and the related effective growth rates are usually much smaller than near the equator.

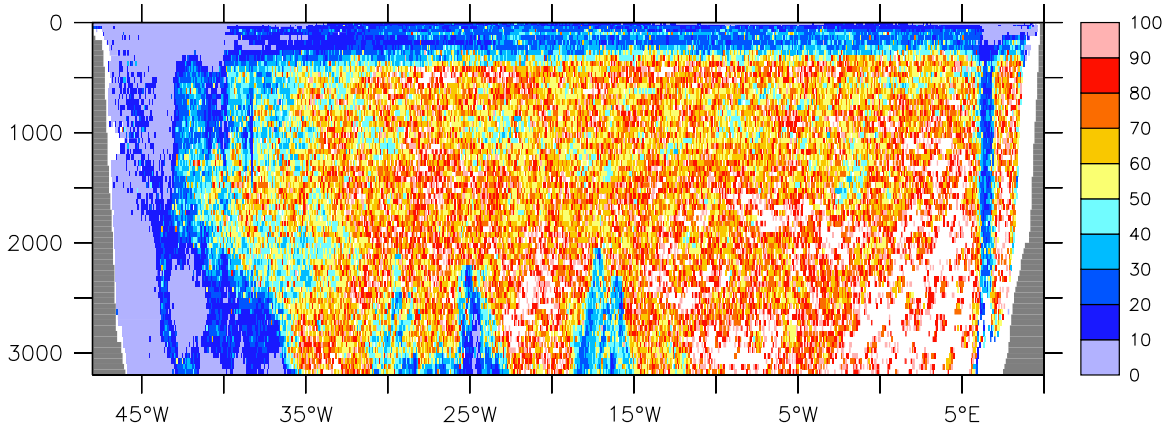

Figure 7. Minimal timescale T in days for symmetric instability near the equator in experiment 1/12–94 (see text for a definition of T). Shown is the long term temporal mean of the minimum of T between 2°N and 2°S.

[26] Large effective growth rates ω^2 correspond to small effective timescales $T = \omega^{-1}$ for the exponential growth of perturbations. In the interior ocean, the smallest, long-term averaged effective timescales T in the region between 2°N and 2°S are in general above 50 d and often are larger than 100 d (Figure 7). This indicates that symmetric instability appears to be an ineffective mechanism for generating fluctuations here as typical damping timescales in the model are of the same order of magnitude. Near the western boundary, however, T can become smaller than 10 d (Figure 7), i.e., much smaller than damping time scales in the model. Note that the meridional and zonal shear associated with the boundary currents (DWBC, NBC) and their variability are responsible for the elevated effective growth rates near the western boundary. Note also that the other model versions also show elevated effective growth rates near the equator with, however, generally smaller amplitudes, consistent with a decreased level of fluctuating energy contained in the high baroclinic modes of these experiments.

[27] The large effective growth rates associated with the western boundary currents and their variability point towards the importance of symmetric instability in generating the stacked jets. However, we note again that the simple linear theory of symmetric instability cannot be directly applied to the equatorial western boundary currents, since the actual equatorial mean flow is more complicated than in the simple theory. On the other hand, the elevated horizontal shear at the equator which is responsible for the large effective growth rates of symmetric instability may also be related to barotropic shear instability. As recently proposed by Hua et al. (submitted manuscript, 2008) and *d'Orgeville et al.* [2007], shear instability of short, low vertical mode Yanai and Rossby waves, generated by a fluctuating DWBC, transfers energy to long, high vertical mode Kelvin waves.

[28] As shown above, the stacked jets in our realistic models are indeed composed of high baroclinic mode Kelvin waves. Furthermore, the models also show pronounced intraseasonal fluctuations near the western boundary at middepths as shown in Figure 8: Wave-like meridional velocity patterns near the DWBC core having maximum amplitudes of about 20 cm s^{-1} at the equator (Figure 8a), periods of about 60 d and westward phase propagation (Figure 8b) are indicative for the presence of short Yanai waves. Such velocity fluctuations were found throughout the whole integration period of the model. Note that the timescale of the simulated fluctuations agree well with the timescale of intraseasonal fluctuations found in current records from 2000 m depth at the western boundary at 44°W near the equator [*Schott et al.*, 1993].

[29] The shear instability of short, low vertical mode Yanai and Rossby waves is accessible to analytical treatment and the results can thus be compared to our model simulations. According to Hua et al. (submitted manuscript, 2008) the meridional wave number l of the perturbation (Kelvin) wave growing on the Yanai wave with zonal wavenumber k is given by $l \approx 0.6\ k$. This meridional wave number l is considered to be equal to the inverse of the corresponding Rossby radius λ_n of the perturbation wave (n denotes the vertical mode number of the Kelvin wave). Using the dispersion relation of a short Yanai wave yields a period $T = 2\pi/\omega = 2\ \pi/(0.6\ \beta\lambda_n)$. Assuming for simplicity a constant stratification of $\bar{N}_0 = 1.71 \times 10^{-3}/s$ (taken from the observations), a Rossby radius of $\lambda_n^2 = N_0\ h_0/(n\pi\beta)$ with $h_0 = 3000$ m and mode number $n = 12$, a period of 73 d and a zonal wave length of 310 km is obtained which is consistent with the characteristics of the Yanai waves found in the model (Figure 8).

5. Discussion and Conclusions

[30] Recent direct current measurements show that the middepth equatorial Atlantic is characterized by high levels of energy contained in zonal flow with high baroclinic mode number (>9). This alternating zonal flow with amplitudes of up to 20 cm s^{-1} is organized in pancake-like structures within ±1° of the equator in the depth-range between 500 m to 2500 m. The stacked jets are present in all ship section from the tropical Atlantic we have analyzed. Individual jets can persist for 1–2 years, but they appear and decay rather irregularly. Using stretched coordinates, we found a pronounced maximum for a wavelength of 625 m in a vertical wave number spectrum. Meridional coherence of zonal

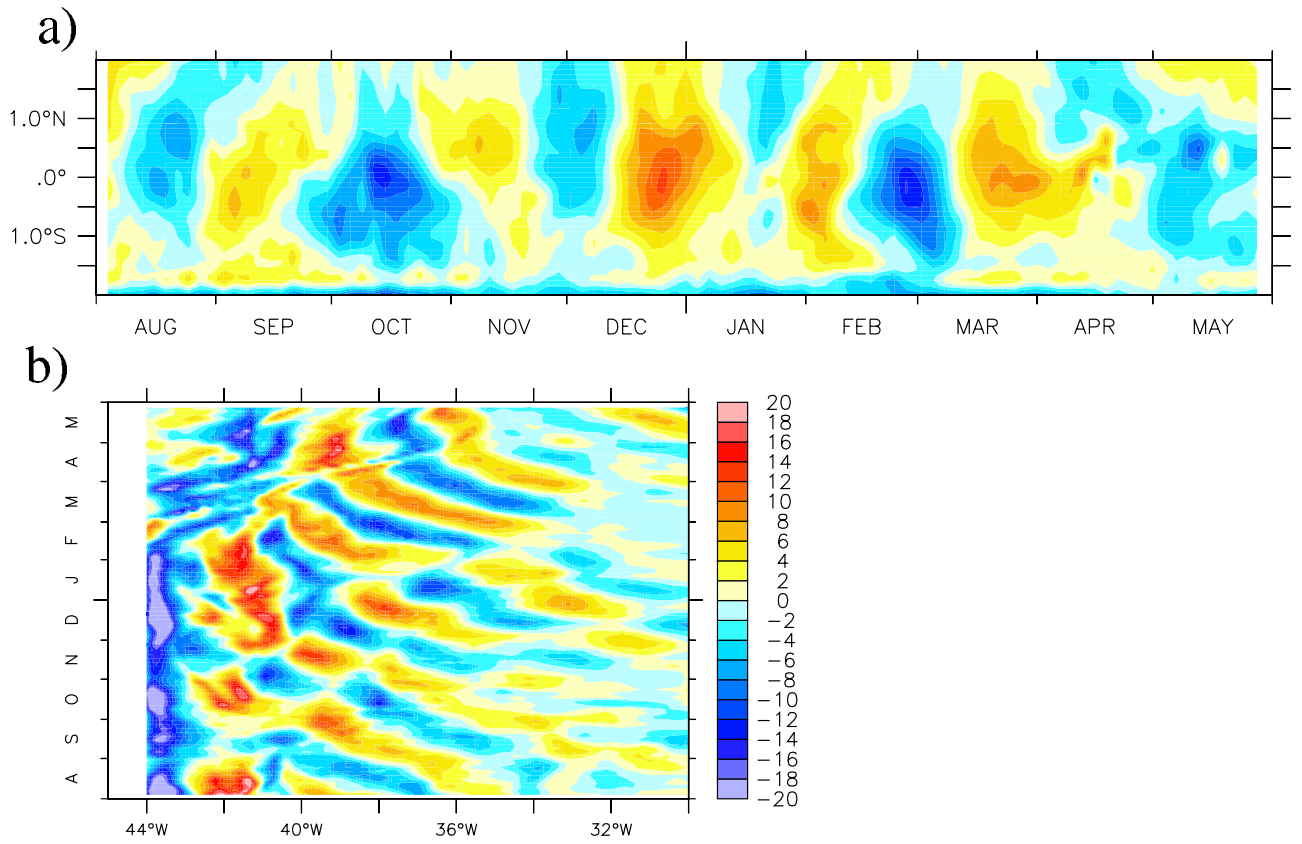

Figure 8. (a) Time series of meridional velocity in cm/s at 38°W at 1900 m depth in experiment 1/12−45. (b) Same as in Figure 8a but at the equator.

velocity, found to be significant within 1° of the equator, also peaks for this wavelength. These findings compare well to results from an analysis of CTD data by *Johnson and Zhang* [2003], who found a maximum wavelength of 660 stretched meters. In their study, the stacked jets were most pronounced at a depth of about 1200 m, which again compares well with the maximum in variance of the stacked jets (Figure 5e) found here.

[31] The equatorial stacked jets can also be found in model simulations. In this study, eddy-permitting and eddy-resolving model versions with very high vertical resolution show that these features are not due to numerical artifacts but grow in amplitude with increasing horizontal and vertical resolution. However, when compared to observations, the strength of the stacked jets is still underestimated by the models we have used. The high baroclinic zonal flow in the models is characterized by eastward wave propagation indicative of high vertical mode Kelvin waves. High levels of energy related to the stacked jets are found in the vicinity of the WBCs (DWBC and NBC) at the equator. Furthermore, depth range and strength of the WBCs in the different experiments are related to depth range and strength of the jets. This model result is supported by the observations: in the equatorial Atlantic, the DWBC is most pronounced in the depth range between 1300−2000 m [*Fischer and Schott*, 1997], and accordingly, stacked jet variance at 35°W peaks in a similar depth range.

[32] It was tested whether the WBCs in the model can become symmetrically unstable due to the elevated meridional and zonal shear of the WBCs present in the vicinity of the equator. Although a direct comparison with simple symmetric instability theory is hampered by the complicated realistic geometry and the nonzonal and strongly fluctuating flow in the equatorial Atlantic, it was shown that effective time scales for inviscid growth of perturbations due to symmetric instability can be as small as a few days. However, simple symmetric instability predicts largest growth rates for small (in inviscid theory for vanishing) vertical wavelengths, which is unrealistic and points towards the need of a consideration of a more realistic mean flow than in simple symmetric instability theory.

[33] All model simulations show elevated levels of horizontal shear related to the western boundary currents and their variability at the equator. As recently suggested by *d'Orgeville et al.* [2007] and Hua et al. (submitted manuscript, 2008), barotropic shear instability of short, low vertical mode (unstable) Yanai and Rossby waves generated by a fluctuating western boundary currents may also be a source for long, high vertical mode Kelvin waves (i.e., the stacked jets). Note that already [*Gill*, 1974] found that short, midlatitude (barotropic) Rossby waves are unstable against perturbations. Hua et al. (submitted manuscript, 2008) extended this work to the equatorial oceans showing that short equatorial (baroclinic) Rossby and Yanai waves are also subject to barotropic instability. In our model simulations, we indeed find energetic short Yanai waves in the region of the DWBC. Furthermore, the modelled stacked jets are composed of high baroclinic mode Kelvin waves.

The scaling of this process, derived from theoretical considerations by Hua et al. (submitted manuscript, 2008), agrees well with the modelled characteristics in respect to wavelength and period of the Yanai wave and vertical mode number of the Kelvin wave. Note that we found the ingredients of the instability mechanism discussed by *d'Orgeville et al.* [2007] and Hua et al. (submitted manuscript, 2008) here in a realistic configuration including a nonvanishing temporal mean of the DWBC, while in the idealised setup of *d'Orgeville et al.* [2007] the DWBC was oscillating with zero temporal mean.

[34] Further support for this generation mechanism comes from observations. At 2000 m depth, energetic intraseasonal fluctuations with periods of 60–70 d have been found in current records from the western boundary near the equator [*Schott et al.*, 1993]. Similar to the Yanai waves in the model, these observations show that the kinetic energy maximum for the 60–70 d band is most pronounced at the equator and to a lesser extend at 1.5°N.

[35] Taking together the observations and the model results, the following generation mechanism of the stacked jets can be hypothesized: The WBCs crossing the equator shows large meridional and zonal shear and produces energetic but unstable Yanai waves of short zonal wave length with eastward group velocity. These short unstable Yanai waves interact and amplify long Kelvin waves. The resulting fluctuations, i.e., high baroclinic mode Kelvin waves, propagate eastward along the equator into the interior and form the stacked jets. Note that the energy transfer from short to large scales is similar to the inverse energy cascade in geostrophic turbulence, but unlike midlatitudes, the resulting fluctuations are of high baroclinic mode. Note also that since the generation mechanism of the stacked jets is given by internal instability (in contrast to external forcing by, e.g., the seasonal cycle), the jets show up and decay irregularly in agreement to the observations.

[36] In the model simulations, momentum flux divergence of the background internal wave field at critical layers as proposed by *Muench and Kunze* [1999] and *Muench and Kunze* [2000] can be ruled out as a forcing mechanism for the stacked jets, because the internal wave field is almost unresolved by the hydrostatic models. We can thus conclude that instability of the large-scale flow is sufficient to generate stacked jets with characteristics that are in agreement with observations. However, as note above, the strength of the stacked jets is underestimated in all model runs, leaving the possibility that transfer of kinetic energy from internal waves to the jets may act to strengthen the jets to the observed levels.

[37] There are strong and deep reaching WBCs crossing the equator in each ocean basin, including the Somali Current in the western equatorial Indian Ocean and the New Guinea Coastal Undercurrent in the western equatorial Pacific Ocean. Instabilities of these WBCs might as well induce fluctuations with high baroclinic mode number, forming the stacked jets in the Pacific and Indian Ocean. However, it is clear that in the tropical Pacific and Indian Ocean, the strength of the DWBC at the equator is much reduced compared to the Atlantic. On the other hand, there is almost no difference in the depth range covered by the stacked jets when comparing the available data from Atlantic, Pacific and Indian Ocean [*Send et al.*, 2002; *Firing*, 1987; *Dengler and Quadfasel*, 2002]. A source of energy for the deep part of the stacked jets might be unsteady or seasonally varying deep western boundary flow across the equator as suggested by *d'Orgeville et al.* [2007] and Hua et al. (submitted manuscript, 2008).

[38] Although the realistic model cannot be directly compared to the idealized situation in theoretical considerations, we find indications that the simulated equatorial Atlantic ocean may often be symmetrically unstable. It is known that symmetric instability is related to (small) secondary closed meridional overturning cells, which lead to static instabilities and thus to strong mixing [*Hua et al.*, 1997; *d'Orgeville et al.*, 2004]. Although it is unlikely that this process is important in the interior equatorial ocean, for which the present model simulations suggests no or weak symmetric instability due to weak background horizontal shear, such overturning and mixing events may be pronounced near the western boundary in the vicinity of the DWBC. Such mixing hot spots could explain deep water-mass modification and abyssal upwelling in the deep equatorial Atlantic as suggested by *Lux et al.* [2001].

[39] **Acknowledgments.** We thank John Toole, Marc d'Orgeville, and Bach Lien Hua for their comments on earlier versions of the manuscript. We are grateful to Fritz Schott and Lothar Stramma for providing the data from the Sonne and Meteor cruises, to Bernard Broules and Yves Gouriou for providing the data from the Etambot 2 and Equalant 1999 cruises, and to Verena Hormann for providing Figure 1a. This study was supported within the Emmy Noether-Program of the Deutsche Forschungsgemeinschaft, the German BMBF as part of the Verbundvorhaben NORDATLANTIK and SOPRAN. The model integrations were performed on a SGI-ALTIX and a NEC-SX8 at the computing centre at the University Kiel, Germany and on a NEC-SX6 at the Deutsches Klimarechenzentrum (DKRZ), Hamburg, Germany.

References

Bourlès, B., et al. (2003), The deep currents in the eastern equatorial Atlantic Ocean, *Geophys. Res. Lett.*, *30*(5), 8002, doi:10.1029/2002GL015095.

Boyer, T. P., and S. Levitus (1997), Objective analyses of temperature and salinity for the world ocean on a 1/4 degree grid, *NOAA Atlas NESDIS 11*, U.S. Gov. Printing Off., Washington, D. C.

Brandt, P., and C. Eden (2005), Annual cycle and interanual variability of the mid-depth tropical Atlantic Ocean, *Deep Sea Res.*, *52*, 199–219.

Dengler, M., and D. Quadfasel (2002), Equatorial deep jets and abyssal mixing in the Indian Ocean, *J. Phys. Oceanogr.*, *32*, 1165–1180.

d'Orgeville, M., B. Hua, R. Schopp, and L. Bunge (2004), Extended deep equatorial layering as a possible imprint of inertial instability, *Geophys. Res. Lett.*, *31*, L22303, doi:10.1029/2004GL020845.

d'Orgeville, M., B. Hua, and H. Sasaki (2007), Equatorial deep jets triggered by a large vertical scale variability within the western boundary layer, *J. Mar. Res.*, *65*, 1–25, doi:10.1357/002224007780388720.

Eden, C. (2006), Mid-depth equatorial tracer tongues in a model of the Atlantic Ocean, *J. Geophys. Res.*, *111*, C12025, doi:10.1029/2006JC003565.

Eden, C., and C. Oschlies (2006), Adiabatic reduction of circulation-related CO_2 air-sea flux biases in North Atlantic carbon-cycle models, *Global Biogeochem. Cycles*, *20*, GB2008, doi:10.1029/2005GB002521.

Emanuel, K. (1994), *Atmospheric Convection*, Oxford Univ. Press, New York.

Eriksen, C. C. (1981), Deep currents and their interpretation as equatorial waves in the western Pacific Ocean, *J. Phys. Oceanogr.*, *11*, 48–70.

Eriksen, C. (1982), Geostrophic equatorial deep jets, *J. Mar. Res.*, *40*, 143–157.

Firing, E. (1987), Deep zonal current in the central equatorial Pacific, *J. Mar. Res.*, *45*, 791–812.

Fischer, J., and F. Schott (1997), Seasonal transport variability of the Deep Western Boundary Current in the equatorial Atlantic, *J. Geophys. Res.*, *102*, 27,751–27,769.

Gill, A. E. (1974), The stability of planetary waves on an infinite beta-plane, *Geophys. Fluid Dyn.*, *6*, 29–47.

Gouriou, Y., B. Bourl, H. Mercier, and R. Chuchla (1999), Deep jets in the equatorial Atlantic Ocean, *J. Geophys. Res.*, *104*, 7865.

Gouriou, Y., C. Andrié, B. Bourlès, S. Freudenthal, S. Arnault, A. Aman, G. Eldin, Y. d. F. Baurand, F. Gallois, and R. Chuchla (2001), Deep

circulation in the equatorial Atlantic Ocean, *Geophys. Res. Lett.*, *28*(5), 819–822.
Haine, T., and J. Marshall (1998), Gravitational, symmetric and baroclinic instability of the ocean mixed layer, *J. Phys. Oceanogr.*, *28*, 634–658.
Hayes, S., and H. Milburn (1980), On the vertical structure of velocity in the eastern equatorial Pacific, *J. Phys. Oceanogr.*, *10*, 633–635.
Hormann, V., and P. Brandt (2007), Atlantic equatorial undercurrent and associated cold tongue variability, *J. Geophys. Res.*, *112*, C06017, doi:10.1029/2006JC003931.
Hua, B. L., D. W. Moore, and S. Le Gentil (1997), Inertial nonlinear equilibrium of equatorial flows, *J. Fluid Mech.*, *331*, 345–371.
Johnson, G. C., and D. Zhang (2003), Structure of the Atlantic Ocean Equatorial Deep Jets, *J. Phys. Oceanogr.*, *33*, 600–609.
Leetma, A., and P. Spain (1981), Results from a velocity transect along the equator from 125° to 159°W, *J. Phys. Oceanogr.*, *11*, 1030–1033.
Levitus, S., and T. P. Boyer (1994), World Ocean Atlas 1994, technical report, U.S. Gov. Print. Off., Washington, D. C.
Lux, M., H. Mercier, and M. Arhan (2001), Interhemispheric exchanges of mass and heat in the Atlantic Ocean in January–March 1993, *Deep Sea Res.*, *48*(3), 605–638.
Luyten, J. R., and J. Swallow (1976), Equatorial undercurrents, *Deep Sea Res.*, *23*, 1005–1007.
McCreary, J. P. (1984), Equatorial beams, *J. Mar. Res.*, *42*, 395–430.
Muench, J. E., and E. Kunze (1999), Internal wave interactions with equatorial deep jets. Part I: Momentum-flux divergence, *J. Phys. Oceanogr.*, *29*, 1453–1467.
Muench, J. E., and E. Kunze (2000), Internal wave interactions with equatorial deep jets. Part II: Acceleration of the jets, *J. Phys. Oceanogr.*, *30*, 2099–2110.
Ponte, R. M. (1989), A simple model of deep equatorial zonal currents forced at lateral boundaries, *J. Phys. Oceanogr.*, *19*, 1881–1891.
Ponte, R., and J. Luyten (1989), Analysis and interpretation of deep equatorial currents in the central Pacific, *J. Phys. Oceanogr.*, *19*, 1025–1038.
Ponte, R., and J. Luyten (1990), Deep velocity measurements in the western equatorial Indian ocean, *J. Phys. Oceanogr.*, *20*, 44–52.
Schmid, C., B. Bourlès, and Y. Gouriou (2005), Impact of the equatorial deep jets on estimates of zonal transport in the Atlantic, *Deep Sea Res.*, *52*, 409–428.
Schott, F., J. Fischer, J. Reppin, and U. Send (1993), On mean and seasonal currents and transports at the western boundary of the equatorial Atlantic, *J. Geophys. Res.*, *98*, 14,353–14,368.
Schott, F., M. Dengler, P. Brandt, K. Affler, J. Fischer, B. Bourles, Y. Gouriou, R. Molinari, and M. Rhein (2003), The zonal transports at 35°W in the tropical Atlantic, *Geophys. Res. Lett.*, *30*(7), 1349, doi:10.1029/2002GL016849.
Send, U., C. Eden, and F. Schott (2002), Atlantic equatorial deep jets: Space-time structure and cross-equatorial fluxes, *J. Phys. Oceanogr.*, *32*(3), 891–902.
Stevens, D. (1983), On symmetric stability and instability of zonal mean flows neat the equator, *J. Atmos. Sci.*, *40*, 882–893.
Stevens, D. P. (1990), On open boundary conditions for three dimensional primitive equation ocean circulation models, *Geophys. Astrophys. Fluid Dyn.*, *51*, 103–133.
Weaver, A. J., and E. S. Sarachik (1990), On the importance of vertical resolution in certain ocean general circulation models, *J. Phys. Oceanogr.*, *20*, 600–609.
Weiss, R., J. L. Bullister, R. H. Gammon, and M. J. Warner (1985), Athomspheric chlorofluoromethanes in the deep equatorial Atlantic, *Nature*, *314*, 608–610.
Wunsch, C. (1977), Response of an equatorial ocean to a periodic monsoon, *J. Phys. Oceanogr.*, *7*, 497–511.

M. Dengler and C. Eden, IFM-GEOMAR, FB I, Ocean Circulation and Climate Dynamics, Düsternbrooker Weg 20, D-24105 Kiel, Germany. (ceden@ifm-geomar.de)